molecular pharmaceutics

ARTICLE

pubs.acs.org/molecularpharmaceutics

Two ^{90}Y-Labeled Multimeric RGD Peptides RGD4 and 3PRGD2 for Integrin Targeted Radionuclide Therapy

Zhaofei Liu,[†,‡,§] Jiyun Shi,[†,‡,§] Bing Jia,[*,†,‡] Zilin Yu,[†,‡] Yan Liu,[†,‡] Huiyun Zhao,[†] Fang Li,[∥] Jie Tian,[⊥] Xiaoyuan Chen,[#] Shuang Liu,[○] and Fan Wang[*,†,‡]

[†]Medical Isotopes Research Center and [‡]Department of Radiation Medicine, Basic Medical Sciences, Peking University, Beijing 100191, China

[∥]Department of Nuclear Medicine, Peking Union Medical College Hospital, Beijing 100857, China

[⊥]Medical Image Processing Group, Institute of Automation, Chinese Academy of Sciences, Beijing 100190, China

[#]Laboratory for Molecular Imaging and Nanomedicine, National Institute of Biomedical Imaging and Bioengineering, National Institutes of Health, Bethesda, Maryland 20892-2281, United States

[○]School of Health Sciences, Purdue University, West Lafayette, Indiana 47907, United States

Supporting Information

ABSTRACT: We have recently developed a series of new Arg-Gly-Asp (RGD) dimeric peptides for specific targeting of integrin $\alpha_v\beta_3$ with enhanced tumor uptake and improved pharmacokinetics. In this study, we investigated ^{90}Y-labeled RGD tetramer (RGD4) and the new type of RGD dimer (3PRGD2), for the radionuclide therapy of integrin $\alpha_v\beta_3$-positive tumors. Biodistribution and gamma imaging studies of ^{111}In labeled RGD4 and 3PRGD2 were performed. Groups of nude mice were used to determine maximum tolerated dose (MTD) of ^{90}Y-DOTA−RGD4 and ^{90}Y-DOTA−3PRGD2. The radionuclide therapeutic efficacy of ^{90}Y-DOTA−RGD4 and ^{90}Y-DOTA−3PRGD2 was evaluated in U87MG tumor-bearing nude mice. The U87MG tumor uptake of ^{111}In-DOTA−3PRGD2 was slightly lower than that of the ^{111}In-DOTA−RGD4 (e.g., 6.13 ± 0.82%ID/g vs 6.43 ± 1.6%ID/g at 4 h post-injection), but the uptake of ^{111}In-DOTA−3PRGD2 in normal organs, such as liver and kidneys, was much lower than that of ^{111}In-DOTA−RGD4, which resulted in much higher tumor-to-nontumor ratios and lower toxicity. The MTD of ^{90}Y-DOTA−RGD4 in nude mice is less than 44.4 MBq, while the MTD of ^{90}Y-DOTA−3PRGD2 in mice is more than 55.5 MBq. ^{90}Y-DOTA−3PRGD2 administration exhibited a similar tumor inhibition effect as compared with ^{90}Y-DOTA−RGD4 at the same dose. The tumor vasculature in the ^{90}Y-DOTA−3PRGD2 treatment group was much less than the control groups. Radionuclide therapy studies exhibited that both ^{90}Y-DOTA−RGD4 and ^{90}Y-DOTA−3PRGD2 caused significant tumor growth delay in the U87MG tumor model. Compared to ^{90}Y-DOTA−RGD4, the low accumulation of ^{90}Y-DOTA−3PRGD2 in normal organs led to lower toxicity and higher MTD in nude mice, which would make it more suitable for high dose or multiple-dose regimens, in order to achieve maximum therapeutic efficacy.

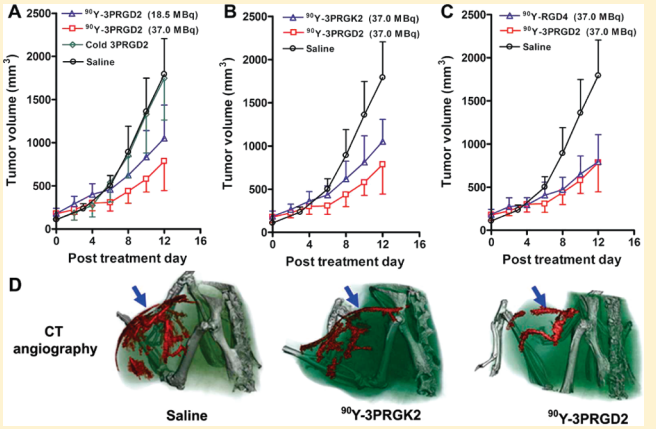

KEYWORDS: integrin $\alpha_v\beta_3$, Arg-Gly-Asp (RGD), ^{90}Y, tumor, radionuclide therapy

INTRODUCTION

Integrin $\alpha_v\beta_3$, one of the integrin family members, is highly expressed on activated endothelial cells, but not resting vessels during angiogenesis, and plays an important role in the regulation of tumor growth, local invasiveness, and metastatic potential.[1] The important role of integrin $\alpha_v\beta_3$ in tumor malignancies has stimulated the extensive investigation of integrin $\alpha_v\beta_3$-targeted noninvasive molecular imaging strategies for early detection of tumors, evaluation of tumor progress, and monitoring treatment efficacy of antiangiogenic drugs.[2,3] In the past decade, a series of Arg-Gly-Asp (RGD) peptide-based probes have been developed for multimodality molecular imaging of integrin $\alpha_v\beta_3$ expression, and several radiolabeled RGD probes have been used in clinical investigation.[4−6]

Received: November 24, 2010
Accepted: January 19, 2011
Revised: January 17, 2011
Published: January 19, 2011

In contrast to the extensive investigation of radiolabeled RGD peptides for tumor imaging purposes, the RGD-based receptor targeted radionuclide therapy is typically rare. Janssen et al. reported, for the first time, the integrin $\alpha_v\beta_3$ targeted radionuclide therapy with ^{90}Y-labeled dimeric RGD peptide E[c(RGDfK)]$_2$ in the NIH:OVCAR-3 subcutaneous (sc) ovarian carcinoma-bearing nude mouse model.[7] A single injection of 37 MBq of ^{90}Y-DOTA−E[c(RGDfK)]$_2$ to mice with small sc tumors caused a significant growth delay as compared with control mice. In a following study, considering the possible low toxicity of monomeric RGD peptides compared with antibody or multimeric RGD peptides, the tumor therapeutic and imaging potential of ^{90}Y/^{111}In-labled monomeric RGD peptide was investigated in a human ovarian carcinoma mouse model, and it was claimed that the RGD monomer can be used for fractionated therapy without evident toxicity.[8]

The promising peptide-based radionuclide therapy relies on the maximized radiation retention in tumors while minimizing the exposure of peptide agents to normal tissues. To increase the tumor uptake of RGD peptides, several groups have proposed the multivalency concept.[9,10] The dimeric or multimeric RGD peptides had almost 1 order of magnitude higher integrin binding affinity than the monomeric analogues, and thus the RGD multimeric tracers gave the higher tumor accumulation at all time points examined as compared to the monomeric RGD peptide probes. A RGD tetrameric peptide was prepared and radiolabeled with ^{64}Cu,[11] and ^{64}Cu-DOTA−RGD tetramer showed significantly higher receptor binding affinity and receptor-mediated tumor uptake than the corresponding monomeric and dimeric RGD analogues, which makes it a promising agent for peptide receptor radionuclide imaging as well as targeted radiotherapy of integrin $\alpha_v\beta_3$-positive tumors.[11] However, the high kidney uptake of the RGD tetramer may limit the further clinical translation due to the possible renal toxicity.

We and collaborators have recently developed a series of new RGD dimers with PEG$_4$ and Gly$_3$ linkers.[12−17] The insertion of the Gly$_3$ or PEG$_4$ spacers significantly increased the distance between the two cyclic RGD peptide motifs, resulting in an increasing in vitro receptor-binding affinity. Importantly, the radiolabeled new types of RGD dimers (e.g., 3PRGD2, see Figure S1 in the Supporting Information) possessed as high tumor uptake as RGD tetramer, but the uptake of the new type of RGD dimers in normal organs was much lower compared with RGD tetramer due to the improved in vivo kinetics.[12,13] Therefore, the new type of RGD dimers are considered to be more promising for targeted radionuclide therapy of integrin $\alpha_v\beta_3$-positive tumors.

In this report, we first investigated the tumor targeting properties and in vivo behaviors of both ^{111}In-labeled RGD tetramer and the new type of RGD dimer (3PRGD2) in the nude mouse models. The receptor-targeted therapeutic potential of the ^{90}Y-labeled RGD tetramer and the new type of RGD dimer (3PRGD2) was then assessed and compared in animal models.

EXPERIMENTAL SECTION

All commercially available chemical reagents were of analytical grade and used without further purification. The bifunctional chelator 1,4,7,10-tetraazadodecane-*N*,*N*′,*N*″,*N*‴-tetraacetic acid (DOTA) was purchased from Macrocyclics, Inc. (Dallas, TX). 1-Ethyl-3-[3-(dimethylamino)propyl]carbodiimide (EDC), *N*-hydroxysulfonosuccinimide (SNHS), and Chelex 100 resin (50−100 mesh) were purchased from Sigma-Aldrich (St. Louis, MO). Water and all buffers were passed through a Chelex 100 column (1 × 15 cm) before use in DOTA conjugation and radiolabeling procedures to ensure that aqueous buffers were metal free. $^{111}InCl_3$ and $^{90}YCl_3$ solutions were obtained from Perkin-Elmer (Norwalk, CT). E[c(RGDfK)]$_2$ (RGD2), PEG$_4$-E[PEG$_4$-c(RGDfK)]$_2$ (3PRGD2) (see Figure S1 in the Supporting Information), E[E[c(RADyK)]$_2$]$_2$ (RAD4) and PEG$_4$-E-[PEG$_4$-c(RGKfD)]$_2$ (3PRGK2: a scrambled control peptide) were obtained from the Peptides International, Inc. (Louisville, KY). The RGD tetramer E[E[c(RGDyK)]$_2$]$_2$ (RGD4) (see Figure S1 in the Supporting Information) was prepared as previously described.[11]

DOTA Conjugation and Radiolabeling. RGD tetramer, the new type of RGD dimer (RGD4 and 3PRGD2), and the control peptides (RGD2, 3PRGK2 and RAD4) were conjugated with chelator DOTA using a previously described method.[11,14,18] Briefly, DOTA was activated by EDC and SNHS for 30 min with a molar ratio of 10:5:4 for DOTA:EDC:SNHS. The DOTA−OSSu (6 μmol, calculated on the basis of *N*-hydroxysulfonosuccinimide) was added to peptides (2 μmol) in 0.1 N $NaHCO_3$ solution (pH 9.0). After being stirred at 4 °C overnight, the DOTA conjugates were isolated by semipreparative HPLC. HPLC analysis and mass spectroscopy were used to confirm the identity of the products. For ^{111}In and ^{90}Y radiolabeling, 74−370 MBq of $^{111}InCl_3$ or $^{90}YCl_3$ was diluted in 300 μL of 0.1 M sodium acetate buffer (pH 5.2) and added to the DOTA−peptide conjugates (5 μg of peptide per mCi of $^{111}InCl_3$ or $^{90}YCl_3$). The reaction mixture was incubated for 20 min at 95 °C, and the ^{111}In or ^{90}Y labeled peptides were then purified by the Sep-Pak C-18 cartridge. The purified products were dissolved in phosphate-buffered saline (PBS) and passed through a 0.22 μm syringe filter for in vivo animal experiments.

Cell Culture and Animal Models. U87MG human glioblastoma cells and HT-29 human colon cancer cells were obtained from American Type Culture Collection (Manassas, VA). U87MG cells were cultured in low glucose Dulbecco's modified Eagle's medium (DMEM), and HT-29 cells were cultured in high glucose DMEM culture medium. Both cell lines were cultured in medium supplemented with 10% (v/v) fetal bovine serum (FBS) at 37 °C in a humidified atmosphere with 5% CO_2. Female BALB/c nude mice (4−5 weeks of age) were purchased from the Department of Experimental Animal, Peking University Health Science Center. U87MG tumor model was established by subcutaneous injection of 2 × 10^6 U87MG tumor cells into the right thighs (for radionuclide therapy studies) or right upper flanks (for biodistribution and scintigraphic imaging studies). HT-29 tumor model was established by subcutaneous injection of 2 × 10^6 HT-29 tumor cells into right thighs (for radionuclide therapy studies) of nude mice. When the tumor volume reached ∼100 mm^3 (2−3 weeks for U87MG, and 1−2 weeks for HT-29 after inoculation), the U87MG and HT-29 tumor-bearing nude mice were used for radionuclide therapy studies. When the tumor volume reached ∼300 mm^3 (3−4 weeks after inoculation), the U87MG tumor-bearing nude mice were used for biodistribution and gamma imaging studies.

Cell Integrin-Receptor Binding Assay. The integrin $\alpha_v\beta_3$ binding affinities of DOTA conjugated RGD and control peptides were determined by cell binding assay. See the Supporting Information for the detailed procedures.

Biodistribution Studies. Female nude mice bearing U87MG xenografts (4 mice per group) were injected with 370 kBq of ^{111}In-DOTA−RGD4 or ^{111}In-DOTA−3PRGD2 via tail vein to evaluate the distribution in major organs of mice. The mice were

sacrificed at 1 h, 4 h, 24 and 72 h postinjection (p.i.). Blood, heart, liver, spleen, kidney, brain, lung, intestine, muscle, bone and tumor were harvested, weighed, and measured for radioactivity in a γ-counter (Wallac 1470-002, Perkin-Elmer, Finland). A group of four U87MG tumor-bearing nude mice was injected with 370 kBq of ^{111}In-DOTA−RAD4 or ^{111}In-DOTA−3PRGK2 as the control, and the biodistribution studies were performed at 4 h p.i. using the same method. Organ uptake was calculated as the percentage of injected dose per gram of tissue (%ID/g). Values were expressed as mean ± SD (n = 4/group).

Gamma-Camera Imaging. For gamma-camera imaging, the U87MG tumor-bearing nude mice were anesthetized with an intraperitoneal injection of sodium pentobarbital at a dose of 45.0 mg/kg. Each animal was administered with ∼13 MBq of the ^{111}In-DOTA−RGD4 or ^{111}In-DOTA−RAD4 in 0.2 mL of saline (n = 3 per group). Animals were placed supine on a two-head γ-camera (GE Infinia Hawkeye) equipped with a parallel-hole, middle-energy, and high-resolution collimator. Anterior images were acquired at 4 and 24 h p.i., and stored digitally in a 128 × 128 matrix. The acquisition count limits were set at 200 k.

Maximum Tolerated Dose (MTD) Studies. The maximum tolerated dose (MTD) of ^{90}Y-DOTA−RGD4 and ^{90}Y-DOTA−3PRGD2 in non-tumor-bearing female BALB/c nude mice was determined by intravenous injection of escalating activities of ^{90}Y-DOTA−RGD4 (11.1, 18.5, 29.6, and 44.4 MBq per mouse), or ^{90}Y-DOTA−3PRGD2 (29.6, 37.0, 44.4, and 55.5 MBq per mouse), respectively (n = 7 per group). Body weight and health status were determined twice weekly over 20 days. Peripheral blood was collected from the tail vein twice weekly and then tested in a blood analyzer for white blood cell (WBC), red blood cell (RBC), platelet (PLT) counts, etc. The MTD was set below the dose that caused severe loss of body weight (>20%) or death of one or more animals of a dose group.

Radionuclide Therapy. To assess the therapeutic potential of ^{90}Y-DOTA−RGD4 or ^{90}Y-DOTA−3PRGD$_2$, U87MG tumor-bearing nude mice with a tumor size of ∼100 mm^3 were randomly assigned to several groups (n = 7 mice per group). Each group was injected via tail vein with single dose injection of saline, cold RGD4 (∼5 μg), cold 3PRGD2 (∼5 μg), ^{90}Y-DOTA−RGD2 (37.0 MBq), ^{90}Y-DOTA−RGD4 (18.5 MBq), ^{90}Y-DOTA−RGD4 (37.0 MBq), ^{90}Y-DOTA−3PRGD2 (18.5 MBq), ^{90}Y-DOTA−3PRGD2 (37.0 MBq), ^{90}Y-DOTA−RAD4 (37.0 MBq), or ^{90}Y-DOTA−3PRGK2 (37.0 MBq) or two doses of ^{90}Y-DOTA−RGD4 (18.5 MBq) (day 0 and day 5). Tumor dimensions were measured twice weekly with digital calipers, and the tumor volume was calculated using the formula volume = $(4/3)\pi[(1/2)\text{ length} \times (1/2)\text{ width} \times (1/2)\text{ height}]$. To monitor potential toxicity, body weight was measured. Mice were euthanized when the tumor size exceeded the volume of 1,500 mm^3 or the body weight lost > 20% of original weight.

To evaluate the efficacy of ^{90}Y-DOTA−RGD4 in low integrin-expressing cancers, two groups of HT-29 tumor-bearing nude mice with a tumor size of ∼100 mm^3 received either 37.0 MBq of ^{90}Y-DOTA−RGD4 or saline. These animals underwent similar tumor and body weight measurement as described above.

Computed Tomography Angiography (CTA). On day 12 after radionuclide therapy of ^{90}Y-DOTA−3PRGD2 (37.0 MBq), the U87MG tumor-bearing nude mice were subjected to CTA to investigate the antiangiogenic effect of the radionuclide therapeutic agents. CTA examinations were performed using a Micro-CT system (Micro-CT-III: developed by Institute of Automation, Chinese Academy of Sciences and Guanzhou Zhongke Kaisheng Medical Technology Co., Ltd.). Mice were examined after being anesthetized with an intraperitoneal injection of sodium pentobarbital at a dose of 45.0 mg/kg. Imaging parameters were as follows: tube voltage, 60 kV; tube current, 1.0 mA (varied automatically according to body size); 600 views, integral time 0.5 s/view. The imaging data was acquired at 5 min after an intravenous injection of 300 μL of iodixanol (Visipaque, 320 mg of iodine/mL; GE Healthcare, Milwaukee, WI, USA). For three-dimensional image reconstruction, the volumetric CT data sets were processed on a separate workstation (Advanced Workstation 4.2, GE Healthcare) with multiplanar reformatting, curved planar reformatting, maximum intensity projection, and volume rendering. The axial source images and the two- and three-dimensional data sets for each of the 3 cases were evaluated.

Immunofluorescence Staining. Frozen U87 tumor tissue slices (7 μm thickness) from the tumor-bearing nude mice on day 12 after radionuclide therapy of ^{90}Y-DOTA−3PRGD2 (37.0 MBq) were fixed with ice-cold acetone, rinsed with PBS and blocked with 10% BSA for 30 min at room temperature. The slices were incubated with rat anti-mouse CD31 (1:100; BD Biosciences) antibody for 1 h at room temperature and then visualized with FITC-conjugated goat anti-rat secondary antibodies (1:200; Jackson Immuno-Research Laboratories, West Grove, PA).

Statistical Analysis. Quantitative data are expressed as means ± SD. Means were compared using one-way analysis of variance (ANOVA) and Student's t test. P values <0.05 were considered statistically significant.

RESULTS

Chemistry and Radiochemistry. The DOTA conjugates of RGD and control peptides were analyzed by both analytical HPLC and mass spectroscopy to confirm the identity of the products. The mass spectroscopy data for DOTA−RGD4 DOTA−3PRGD2, DOTA−RGD2, and DOTA−3PRGK2 have been reported previously.[11,14,19,20] The electrospray ionization mass spectrometry (ESI-MS) of DOTA−RAD4 was m/z = 3255.58 for $[M + H]^+$ (3255.48 calcd for $[C_{143}H_{214}N_{43}O_{45}]^+$). After labeling and purification, the specific activity of ^{111}In and ^{90}Y tracers was typically about 7.4−14.8 MBq/nmol (0.2−0.4 Ci/mmol), with radiochemical purity greater than 98% as determined by analytic radio-HPLC.

Biodistribution Studies. To investigate the in vivo behavior of ^{111}In-DOTA−RGD4 and ^{111}In-DOTA−3PRGD2, we performed biodistribution studies in female BALB/c nude mice bearing U87MG tumor xenografts. ^{111}In-DOTA−RGD4 depicted a similar biodistribution pattern with previously reported ^{111}In-labeled RGD tetramer ^{111}In-DOTA−E[E[c(RGDfK)]$_2$]$_2$.[21] As shown in Figure 1A, the uptake of ^{111}In-DOTA−RGD4 in U87MG tumors was 7.35 ± 0.62%ID/g at 1 h p.i., which was decreased to 6.43 ± 1.60%ID/g, 3.67 ± 0.57%ID/g, and 1.72 ± 0.41%ID/g at 4 h, 24 h, and 72 h p.i., respectively (n = 4/group). ^{111}In-DOTA−RGD4 was cleared predominantly through the renal pathway as evidenced by higher kidney uptake at early time points (13.23 ± 1.22%ID/g and 10.99 ± 0.88%ID/g at 1 and 4 h p.i., respectively). The other organs such as heart, muscle, and brain showed very low uptake. The high intestine uptake of the radioprobe was also observed, with 5.93 ± 1.00%ID/g and 5.09 ± 0.76%ID/g at 1 and 4 h p.i., respectively. ^{111}In-DOTA−3PRGD2 also showed rapid blood clearance. The uptake of ^{111}In-DOTA−3PRGD2 in U87MG tumors was 5.62 ± 0.88%ID/g, 6.13 ± 0.82%ID/g, 2.03 ± 0.24%ID/g, and

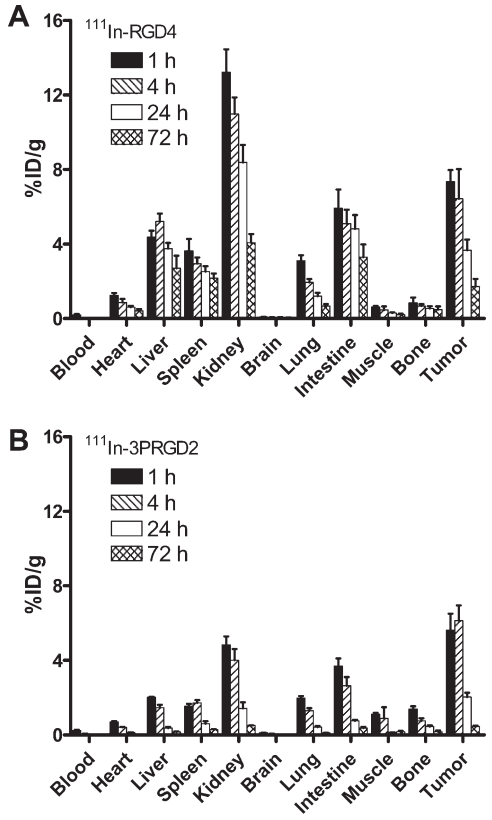

Figure 1. (A) Biodistribution of ^{111}In-DOTA−RGD4 (^{111}In-RGD4) in U87MG tumor-bearing nude mice at 1 h, 4 h, 24 h, and 72 h after injection (370 kBq per mouse). (B) Biodistribution of ^{111}In-DOTA−3PRGD2 (^{111}In-3PRGD2) in U87MG tumor-bearing nude mice at 1 h, 4 h, 24 h, and 72 h after injection (370 kBq per mouse). Data are expressed as %ID/g ± SD (n = 4 per group).

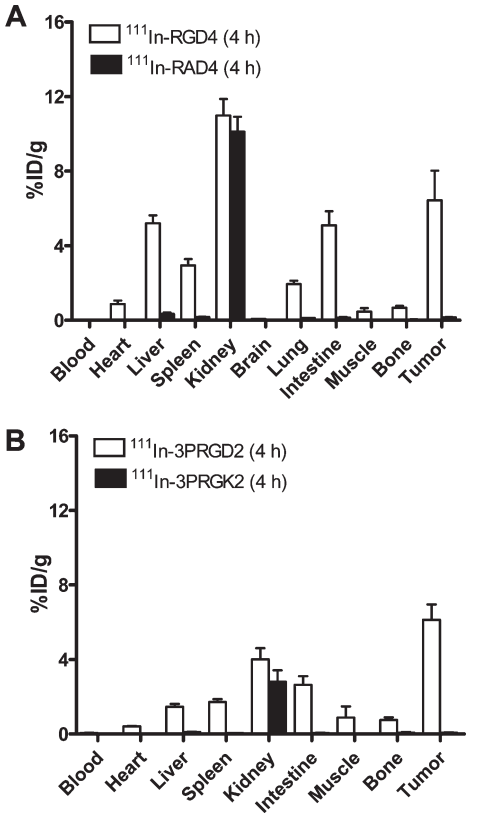

Figure 2. (A) Comparison of biodistribution of ^{111}In-DOTA−RGD4 (^{111}In-RGD4) and ^{111}In-DOTA−RAD4 (^{111}In-RAD4) in U87MG tumor-bearing nude mice at 4 h after injection (370 kBq per mouse). (B) Comparison of biodistribution of ^{111}In-DOTA−3PRGD2 (^{111}In-3PRGD2) and ^{111}In-DOTA−3PRGK2 (^{111}In-3PRGK2) in U87MG tumor-bearing nude mice at 4 h after injection (370 kBq per mouse). Data are expressed as %ID/g ± SD (n = 4 per group).

0.45 ± 0.05%ID/g at 1 h, 4 h, 24 h, and 72 h p.i., respectively (n = 4/group). The tumor uptake of ^{111}In-DOTA−3PRGD2 was all slightly lower than that of the ^{111}In-DOTA−RGD4, but the uptake of ^{111}In-DOTA−3PRGD2 in normal organs, such as liver and kidneys, was much lower than that of ^{111}In-DOTA−RGD4 (P < 0.05, see Figure S4 in the Supporting Information), which resulted in much higher tumor-to-nontumor ratios (P < 0.05, see Figure S5 in the Supporting Information).

Integrin receptor specificity of ^{111}In-DOTA−RGD4 and ^{111}In-DOTA−3PRGD2 was demonstrated by the experiments with injection of the ^{111}In-DOTA−RAD4 and ^{111}In-DOTA−3PRGK2. The tumor uptake of ^{111}In-DOTA−RAD4 and ^{111}In-DOTA−3PRGK2 at 4 h p.i. was significantly lower than that of the ^{111}In-DOTA−RGD4 and ^{111}In-DOTA−3PRGD2 (P< 0.001, Figure 2A,B), indicating the receptor-mediated targeting of ^{111}In-DOTA−RGD4 and ^{111}In-DOTA−3PRGD2 in integrin-positive U87MG tumors.

Gamma-Camera Imaging. Representative planar γ-images of U87MG tumor-bearing mice at 4 and 24 h after intravenous injection of ~13 MBq of ^{111}In-DOTA−RGD4 and ^{111}In-DOTA−RAD4 are shown in Figure 3. The U87MG tumors receiving ^{111}In-DOTA−RGD4 were clearly visible at 4 and 24 h p.i., with high contrast to the contralateral background. Prominent renal uptake of the probe was also observed. The U87MG tumors were undetectable in the nude mice after the intravenous injection of ~13 MBq of ^{111}In-DOTA−RAD4. ^{111}In-RAD4 also showed high renal uptake in the U87MG tumor-bearing mice, suggesting the renal clearance of the probe.

Maximum Tolerated Dose (MTD) Studies. For MTD determination, non-tumor-bearing mice were separated into several groups, each of which underwent an escalating single injection dose of ^{90}Y-RGD4 or ^{90}Y-3PRGD2. Animal body weight, WBC, RBC, and platelet counts were analyzed after injection (Tables 1 and 2, see Figures S6 and S7 in the Supporting Information). A dose-dependent reduction of WBC was observed. On day 12 p.i., the WBC reached the lowest level and then recovered gradually to the baseline. Animals in the 44.4 MBq ^{90}Y-DOTA−RGD4 group experienced a reduction of WBC to 13.34 ± 4.31% of the original value on day 12 p.i. (Table 1). All other groups maintained a varying degree of reducing WBC with the 29.6 MBq group to 30.17 ± 16.15 %, the 18.5 MBq group to 42.48 ± 14.41 %, and the 11.1 MBq group to 67.08 ± 12.28 % on day 12 p.i., respectively. There was no significant reduction of RBC counts in all groups injected with various doses of ^{90}Y-DOTA−RGD4. Platelet counts revealed a rapid toxicity in the first 10 days, and then recovered on day 19 p.i. (see Figure S6 in the Supporting Information). No significant body weight difference was observed among the 11.1 MBq, 18.5 MBq and 29.6 MBq groups. However, significant body weight loss (>20% of the original) was observed in the 44.4 MBq group on day 5 p.i. Overall, animals that received 44.4 MBq of ^{90}Y-DOTA−RGD4 experienced a

maximum reduction in WBC counts and body weight. The MTD of ^{90}Y-DOTA−RGD4 in mice is less than 44.4 MBq.

A dose-dependent reduction of WBC for ^{90}Y-DOTA−3PRGD2 was also observed. On day 11 p.i., the WBC reached the lowest level and then recovered gradually to the baseline. Animals in the 55.5 MBq ^{90}Y-DOTA−3PRGD2 group experienced a reduction of WBC to 28.14 ± 9.41 % of the original value on day 11 p.i. (Table 2). All other groups maintained a varying degree of reducing WBC, with the 44.4 MBq group to 30.35 ± 16.94 %, the 37.0 MBq group to 32.67 ± 15.55 %, and the 29.6 MBq group to 49.70 ± 15.23 % on day 11 p.i., respectively. There was no significant reduction of WBC counts in the saline group (Table 2). Platelet counts revealed a rapid toxicity in the first 10 days, and then recovered on day 18 p.i. (see Figure S7 in the Supporting Information). No significant body weight loss (>20% of the original) was observed among the 29.6 MBq, 37.0 MBq. 44.4 MBq and 55.5 MBq groups. Overall, there was no mortality in all groups, and the WBC counts were recovered on day 18 p.i. The 55.5 MBq did not reach the MTD of ^{90}Y-DOTA−3PRGD2 in mice.

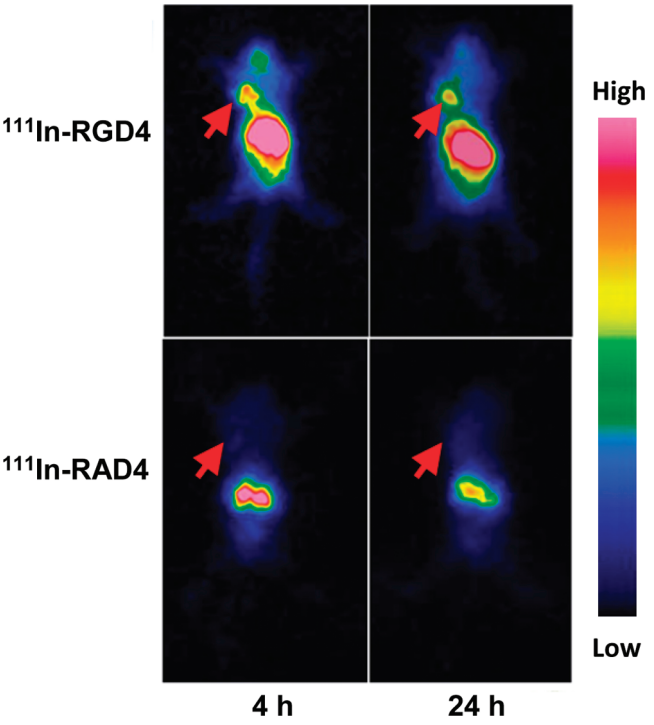

Figure 3. Representative planar gamma images of U87MG tumor-bearing nude mice at 4 and 24 h after intravenous injection of ~13 MBq ^{111}In-DOTA−RGD4 (^{111}In-RGD4) or ^{111}In-DOTA−RAD4 (^{111}In-RAD4). (n = 3 per group). Tumors are indicated by red arrows.

Peptide Receptor Radionuclide Therapy. The therapeutic efficacy of ^{90}Y-DOTA−RGD4 or ^{90}Y-DOTA−3PRGD2 was investigated in integrin-positive U87MG tumor-bearing nude mice. ^{90}Y-DOTA−RGD4 possessed an enhanced tumor inhibition effect as compared with ^{90}Y-DOTA−RGD2 at day 12 (P < 0.05, Figure 4A), which was most likely caused by the significantly increased tumor uptake of ^{90}Y-DOTA−RGD4 compared to ^{90}Y-DOTA−RGD2.[11] The significantly increased antitumor efficacy of ^{90}Y-DOTA−RGD4 as compared with ^{90}Y-DOTA−RAD4 at day 12 (P < 0.01, Figure 4A) demonstrated the integrin-specific therapy of ^{90}Y-DOTA−RGD4. The therapeutic efficacy of ^{90}Y-DOTA−RGD4 appeared to be dose dependent. The tumor growth rate decreased after a single dose of 37.0 MBq ^{90}Y-DOTA−RGD4, which was more pronounced than that of 18.5 MBq ^{90}Y-DOTA−RGD4 at day 9 (P < 0.05, Figure 4B). The cold RGD4 did not show any antitumor effect (Figure 4B). From day 8, the mice receiving the 2 × 18.5 MBq dose regimen of ^{90}Y-DOTA−RGD4 exhibited the much better tumor growth inhibition as compared with the 18.5 MBq single dose (P < 0.01, Figure 4C). The therapeutic efficacy of ^{90}Y-DOTA−RGD4 was also examined in HT-29 human colon cancer xenografts, and the result is shown in Figure 4D. ^{90}Y-DOTA−RGD4 administration exhibited a tumor inhibition effect in the treatment group as compared with the saline control group. However, the tumor growth

Table 1. WBC Variations on Different Days after Injection of ^{90}Y-DOTA−RGD4

	WBC[a]				
dose (MBq)	day 5	day 9	day 12	day 16	day 19
44.4	25.31 ± 8.13	18.71 ± 9.50	13.34 ± 4.31	47.10 ± 17.63	123.15 ± 77.38
29.6	42.62 ± 19.79	48.99 ± 38.01	30.17 ± 16.15	53.31 ± 26.02	107.26 ± 39.94
18.5	61.60 ± 26.48	79.45 ± 40.03	42.48 ± 14.41	70.49 ± 32.24	101.80 ± 33.56
11.1	103.82 ± 41.33	100.38 ± 34.90	67.08 ± 12.28	101.37 ± 25.73	156.78 ± 28.02

[a] Data are expressed as percentage of original values.

Table 2. WBC Variations on Different Days after Injection of ^{90}Y-DOTA−3PRGD2

	WBC[a]				
dose (MBq)	day 4	day 8	day 11	day 15	day 18
55.5	40.40 ± 13.16	29.10 ± 23.73	28.14 ± 9.41	67.68 ± 11.59	97.29 ± 26.71
44.4	34.20 ± 17.62	32.82 ± 14.50	30.35 ± 16.94	65.19 ± 16.01	102.78 ± 21.72
37.0	43.64 ± 10.80	42.14 ± 23.66	32.67 ± 15.55	71.61 ± 22.20	106.34 ± 15.13
29.6	56.49 ± 14.24	67.64 ± 25.92	49.70 ± 15.23	83.67 ± 23.97	105.04 ± 35.31
0	100.74 ± 24.71	110.43 ± 26.20	118.45 ± 12.35	106.88 ± 7.56	106.34 ± 12.29

[a] Data are expressed as percentage of original values.

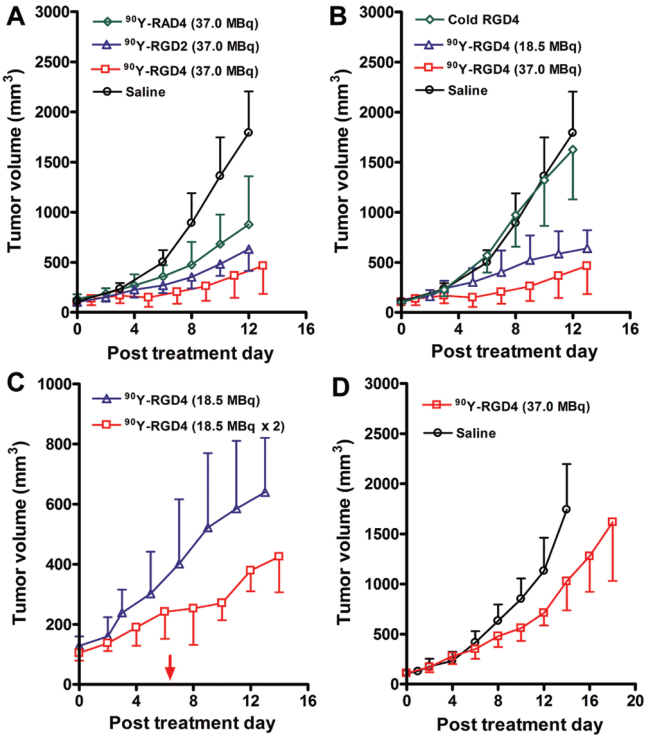

Figure 4. (A) Radionuclide therapy of established U87MG tumors in nude mice with saline, ^{90}Y-DOTA−RAD4 (^{90}Y-RAD4, 37.0 MBq), ^{90}Y-DOTA−RGD2 (^{90}Y-RGD2, 37.0 MBq), or ^{90}Y-DOTA−RGD4 (^{90}Y-RGD4, 37.0 MBq). (B) Radionuclide therapy of established U87MG tumors in nude mice with saline, cold RGD4 (~5 μg), ^{90}Y-DOTA−RGD4 (18.5 MBq), or ^{90}Y-DOTA−RGD4 (37.0 MBq). (C) Radionuclide therapy of established U87MG tumors in nude mice with a single dose (18.5 MBq) or two doses (18.5 MBq on day 0 and day 5, respectively) of ^{90}Y-DOTA−RGD4. The second administration time point is indicated by an arrow. (D) Radionuclide therapy of established HT-29 tumors (low integrin expression) in nude mice with saline or ^{90}Y-DOTA−RGD4 (37.0 MBq). Volume of tumors in each treatment group was measured and expressed as a function of time (means ± SD, n = 7 per group).

of the HT-29 nude mice injected with ^{90}Y-DOTA−RGD4 was rather rapid, with the tumor size reaching over 1500 mm^3 on day 18 posttreatment.

The therapeutic efficacy of ^{90}Y-DOTA−3PRGD2 was also determined in U87MG tumor bearing nude mice. As shown in Figure 5A, the cold 3PRGD2 did not caused any antitumor effect. The tumor growth rate decreased after a single dose of 37.0 MBq ^{90}Y-DOTA−3PRGD2, which was more pronounced than that of 18.5 MBq ^{90}Y-DOTA−3PRGD2 at day 10 ($P < 0.05$). From day 8, the tumor growth inhibition effect of ^{90}Y-DOTA−3PRGD2 was much better than that of ^{90}Y-DOTA−3PRGK2 due to the specific receptor targeting ($P < 0.05$, Figure 5B). ^{90}Y-DOTA−3PRGD2 administration exhibited a similar tumor inhibition effect as compared with ^{90}Y-DOTA−RGD4 at the same dose (Figure 5C).

Computed Tomography Angiography (CTA). The tumor vasculature status after radionuclide therapy with ^{90}Y-DOTA−3PRGD2 was examined by CTA using a Micro-CT system. Combined 3D surface rendering demonstrates the major tumor feeder vessels (TV) visible (Figure 6). The vasculature in the control group grew significantly larger in diameter and higher in density in comparison to that in the ^{90}Y-DOTA−3PRGK2 and ^{90}Y-DOTA−3PRGD2 groups. The tumor vasculature in the ^{90}Y-DOTA−3PRGD2 group was significantly inhibited as compared with saline and ^{90}Y-DOTA−3PRGK2 groups.

Immunofluorescence Staining. CD31 was measured by immunofluorescence staining to validate the ex vivo tumor vasculature status. Consistent with the CTA data, the tumor vasculature in the ^{90}Y-DOTA−3PRGD2 treatment group is much less than that in the control groups (Figure 6), demonstrating the vasculature damage of ^{90}Y-DOTA−3PRGD2.

DISCUSSION

This study was designed to evaluate ^{90}Y-labeled RGD tetrameric peptide and the new type of RGD dimeric peptide as therapeutic agents for integrin-positive tumors. The results presented show that, in the experimental model, ^{90}Y-DOTA−RGD4 and ^{90}Y-DOTA−3PRGD2 exhibited a markedly enhanced therapeutic effect, compared with the dimeric ^{90}Y-DOTA−RGD2, ^{90}Y-labeled scrambled control peptides, and the cold peptides.

The multimer concept has been previously applied to develop dimeric, tetrameric, and even octameric RGD peptides for improved tumor targeting over the corresponding monomeric RGD peptide analogues.[19,22−24] The multimeric RGD peptide tracers showed higher receptor-binding affinity and specificity to integrin $\alpha_v\beta_3$ in vitro and enhanced tumor uptake and retention in vivo as compared with the monomeric RGD peptides. Unfortunately, as the peptide multiplicity increases, the uptake of radiolabeled multimeric RGD peptides in normal organs, especially in the kidneys, is also significantly increased. In addition, the cost for the preparation of RGD tetramer and RGD octamer is prohibitively high. Thus, an alternative approach is needed to improve integrin-targeting capability and minimize the radiotracer accumulation in normal organs, as well as reduce the cost. In this study, we evaluated the in vitro and in vivo integrin receptor binding characteristics of RGD tetramer (RGD4) and the new type of RGD dimer (3PRGD2). DOTA−RGD4 possessed significantly increased integrin binding affinity as compared with the RGD dimer (DOTA−RGD2), and the new type of RGD dimer (DOTA−3PRGD2) depicted the similar binding affinity like DOTA−RGD4 (see Figure S2 in the Supporting Information). ^{111}In-DOTA−3PRGD2 exhibited comparable tumor uptake with ^{111}In-DOTA−RGD4 in the integrin-positive U87MG tumors. The normal organ uptake (e.g., kidney and liver) of ^{111}In-DOTA−3PRGD2, however, was significantly lower than that of ^{111}In-DOTA−RGD4, which resulted in better tumor-to-nontumor contrast and possibly much lower toxicity.

Hematological parameters and body weight loss were used as the gross toxicity criterion in our MTD study. For ^{90}Y-DOTA−RGD4, of the doses chosen for evaluation, 44.4 MBq resulted in profound animal body weight loss (>20% of the original) between 3 and 10 days after administration. Doses of 29.6 MBq and less did not produce animal death or any statistical difference in body weight (see Figures S6 and S8 in the Supporting Information). For ^{90}Y-DOTA−3PRGD2, of the doses chosen for evaluation, the maximum dose of 55.5 MBq did not lead to profound animal body weight loss in the whole examination period (see Figures S7 and S8 in the Supporting Information). All the radiation doses of ^{90}Y-DOTA−RGD4 and ^{90}Y-DOTA−3PRGD2 caused evident decrease of the WBC and PLT counts; however, almost all of them were recovered by the end of the observation period (~20 days postinjection). Based on the MTD data, we can speculate that the MTD for ^{90}Y-DOTA−RGD4 is less than 44.4 MBq while the MTD for ^{90}Y-DOTA−3PRGD2 is higher

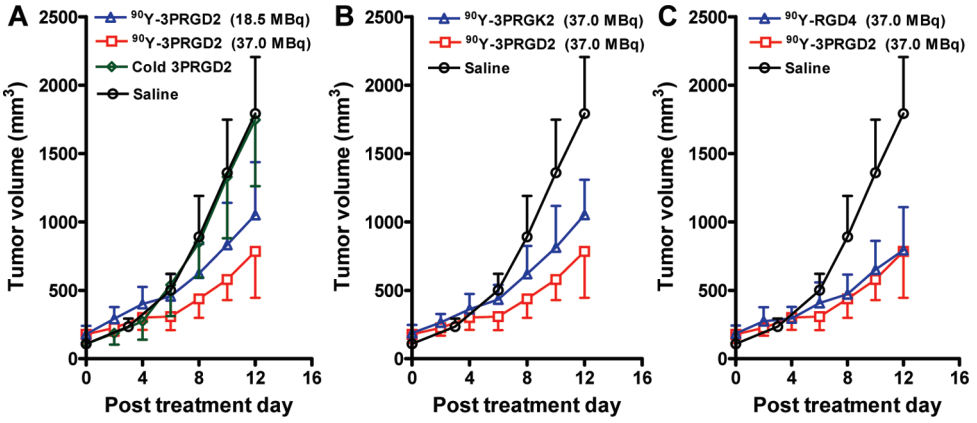

Figure 5. (A) Radionuclide therapy of established U87MG tumors in nude mice with saline, cold 3PRGD2, ^{90}Y-DOTA−3PRGD2 (^{90}Y-3PRGD2, 18.5 MBq), or ^{90}Y-DOTA−3PRGD2 (37.0 MBq). (B) Radionuclide therapy of established U87MG tumors in nude mice with saline, ^{90}Y-DOTA−3PRGD2 (37.0 MBq) or ^{90}Y-DOTA−3PRGK2 (^{90}Y-3PRGK2, 37.0 MBq). (C) Radionuclide therapy of established U87MG tumors in nude mice with saline, ^{90}Y-DOTA−RGD4 (^{90}Y-RGD4, 37.0 MBq), or ^{90}Y-DOTA−3PRGD2 (37.0 MBq).Volume of tumors in each treatment group was measured and expressed as a function of time (means ± SD, n = 7 per group).

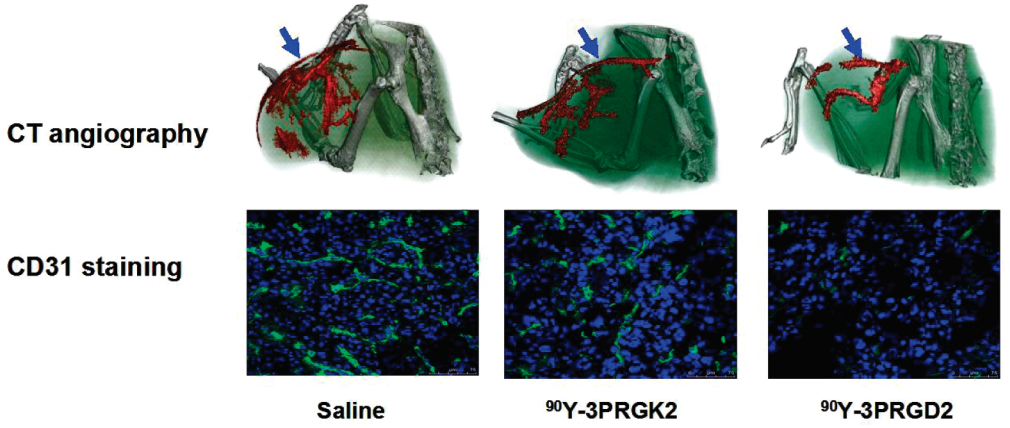

Figure 6. (Top) CT angiography examination of U87MG tumor-bearing nude mice on day 12 after treatment with saline, ^{90}Y-DOTA−3PRGK2 (^{90}Y-3PRGK2, 37.0 MBq), or ^{90}Y-DOTA−3PRGD2 (^{90}Y-3PRGD2, 37.0MBq). (Bottom) CD31 staining of the frozen U87MG tumor tissue slices from the tumor-bearing nude mice on day 12 after treatment with saline, ^{90}Y-DOTA−3PRGK2 (37.0 MBq), or ^{90}Y-DOTA−3PRGD2 (37.0 MBq). The tumors are indicated by arrows.

than 55.5 MBq. Mice exhibited much higher tolerance to ^{90}Y-DOTA−3PRGD2 as compared with ^{90}Y-DOTA−RGD4, which is most likely due to the rather rapid clearance and low uptake of ^{90}Y-DOTA−3PRGD2 in normal organs, especially in the kidneys and liver. Janssen et al.[7] set the MTD of ^{90}Y-labed dimeric RGD peptide (^{90}Y-DOTA−RGD2) in nontumor nude mice at the dose of 37 MBq based on their MTD studies. The new type of RGD dimeric peptide ^{90}Y-DOTA−3PRGD2 exhibited higher MTD in nude mice than that of ^{90}Y-DOTA−RGD2. The higher MTD would allow higher single dose administration, and also possible treatment regimen of multiple doses.

Radiolabeled RGD peptides can specifically bind integrin $\alpha_v\beta_3$ expressed both on tumor cell surface and the new-born tumor vasculature,[25] therefore, ^{90}Y-labeled RGD peptides are considered to specifically deliver radiotherapeutics to both the integrin $\alpha_v\beta_3$-expressing tumor cells and the tumor neovasculature, which may lead to better management of solid tumors. In our radionuclide therapy studies, partial tumor regression was successfully achieved by a single dose of 37 MBq of ^{90}Y-DOTA−RGD4, and the therapeutic effect of ^{90}Y-DOTA−RGD4 was significantly better than those of ^{90}Y-DOTA−RAD4 and ^{90}Y-DOTA−RGD2 (Figure 4A). To evaluate the integrin specific targeting of ^{90}Y-DOTA−RGD4, we performed the therapy study in a HT-29 human colon tumor model, in which tumor cells express a very low level of integrin $\alpha_v\beta_3$, while the new-born tumor vasculature expressed a moderate level of integrin $\alpha_v\beta_3$.[25,26] It was found that the therapeutic efficacy of ^{90}Y-DOTA−RGD4 was not evident, due to the low expression of integrin $\alpha_v\beta_3$ on HT-29 cells (Figure 4D). Yoshimoto et al.[8] reported that multiple-dose administration (11.1 MBq × 3) of ^{90}Y-DOTA−c(RGDfK) induced significant inhibition of tumor growth compared with single dose injection. We also investigated the fractionated dose administration of ^{90}Y-DOTA−RGD4 in U87MG tumor model. Two doses of ^{90}Y-DOTA−RGD4 significantly increased the antitumor effect as compared with the single dose, although two dose administration of ^{90}Y-DOTA−RGD4 still could not fully inhibit the tumor growth (Figure 4C). Due to the similar tumor uptake and tumor radiation retention, ^{90}Y-DOTA−3PRGD2 possessed a comparable tumor regression effect as compared with ^{90}Y-DOTA−RGD4 (Figure 5C) at the same dose. Considering the lesser toxicity of ^{90}Y-DOTA−3PRGD2, the higher or multiple-dose injection of ^{90}Y-DOTA−3PRGD2 is speculated to be more effective for tumor therapy. The

dx.doi.org/10.1021/mp100403y |*Mol. Pharmaceutics* 2011, 8, 591–599

antiangiogenic effect of ^{90}Y-DOTA−3PRGD2 resulted in reduced tumor vasculature as determined by CTA analysis. Similarly, CD31+ vascular endothelial cells were also significantly reduced, suggesting tumor regression and vasculature collapse (Figure 6).

Several options can be explored to optimize the therapeutic efficacy with radiolabeled RGD peptides, such as repeated injection or the combination with other approaches (e.g., chemotherapy), as well as the selection of more suitable radioisotopes like ^{177}Lu (Emax, 0.497 MeV; half-life, 6.7 days). In addition, more clinically relevant tumor models such as orthotopic or spontaneous tumor models may be needed for further investigation of ^{90}Y-labeled RGD peptides as promising agents for both tumor cell and tumor vasculature targeted radionuclide therapy.

CONCLUSION

Both ^{111}In-DOTA−RGD4 and ^{111}In-DOTA−3PRGD2 exhibited specific tumor targeting properties, but the uptake of ^{111}In-DOTA−3PRGD2 in normal organs, especially kidneys and liver, was significantly reduced, most likely resulting from the improved in vivo kinetics. The low accumulation in normal organs must lead to lower toxicity and higher MTD of ^{90}Y-DOTA−3PRGD2 in nontumor nude mice. Radionuclide therapy studies exhibited that both ^{90}Y-DOTA−RGD4 and ^{90}Y-DOTA−3PRGD2 caused significant tumor growth delay in the nude mice bearing U87MG tumor xenografts. The higher MTD of ^{90}Y-DOTA−3PRGD2 would make it more suitable for high dose or multiple-dose regimens, in order to achieve maximum therapeutic efficacy.

ASSOCIATED CONTENT

Supporting Information. Additional methods; chemical structures of DOTA−RGD2, DOTA−RGD4 and DOTA−3PRGD2; cell binding assay of DOTA−RGK2, c(RGDyK), DOTA−RGD2, DOTA−RGD4, and DOTA−3PRGD2; representative planar gamma images of U87MG tumor-bearing nude mice after intravenous injection of ^{111}In-DOTA−3PRGD2; comparison of uptake values between ^{111}In-DOTA−RGD4 and ^{111}In-DOTA−3PRGD2 in the blood, liver, kidney, and U87MG tumor at 1 h, 4 h, 24 h, and 72 h postinjection; comparison of tumor-to-liver and tumor-to-kidney ratios between ^{111}In-DOTA−RGD4 and ^{111}In-DOTA−3PRGD2 at 1 h, 4 h, 24 h, and 72 h postinjection in the U87MG tumor-bearing mice; blood cells and body weight changes of nude mice receiving saline or different doses of ^{90}Y-DOTA−RGD4 or ^{90}Y-DOTA−3PRGD2; body weight changes of U87MG tumor-bearing nude mice receiving saline, ^{90}Y-DOTA−RGD2 (37.0 MBq), ^{90}Y-DOTA−RGD4 (18.5 MBq), or ^{90}Y-DOTA−RGD4 (37.0 MBq); body weight changes of U87MG tumor-bearing nude mice receiving saline, ^{90}Y-DOTA−RGD4 (37.0 MBq), ^{90}Y-DOTA−3PRGK2 (37.0 MBq), ^{90}Y-DOTA−3PRGD2 (18.5 MBq), or ^{90}Y-DOTA−3PRGD2 (37.0 MBq). This material is available free of charge via the Internet at http://pubs.acs.org.

AUTHOR INFORMATION

Corresponding Author

*Medical Isotopes Research Center, Peking University, 38 Xueyuan Rd, Beijing 100191, China. F.W.: tel and fax, 86-10-82801145; e-mail, wangfan@bjmu.edu.cn. B.J.: tel, 86-10-82802871; fax, 86-10-82801145; e-mail, jiabing@bjmu.edu.cn.

Author Contributions

§These authors contributed equally to this work.

ACKNOWLEDGMENT

This work was supported, in part, by NSFC projects (30870728, 30930030, 30900373, 81000625, and 81028009), an "863" project (2007AA02Z467), a "973" project (2011CB707703), and grants from the Ministry of Science and Technology of China (2009ZX09103-733, 2009ZX09301-010 and 2009ZX09103-746). Parts of this manuscript were presented at the Society of Nuclear Medicine (SNM) Annual Meeting in Toronto, Canada, June 13−17, 2009.

REFERENCES

(1) Kumar, C. C. Integrin alpha v beta 3 as a therapeutic target for blocking tumor-induced angiogenesis. *Curr. Drug Targets* **2003**, *4* (2), 123–31.

(2) Cai, W.; Chen, X. Multimodality molecular imaging of tumor angiogenesis. *J. Nucl. Med.* **2008**, *49* (Suppl. 2), 113S–28S.

(3) Cai, W.; Niu, G.; Chen, X. Imaging of integrins as biomarkers for tumor angiogenesis. *Curr. Pharm. Des.* **2008**, *14* (28), 2943–73.

(4) Beer, A. J.; Haubner, R.; Sarbia, M.; Goebel, M.; Luderschmidt, S.; Grosu, A. L.; Schnell, O.; Niemeyer, M.; Kessler, H.; Wester, H. J.; Weber, W. A.; Schwaiger, M. Positron emission tomography using [^{18}F]Galacto-RGD identifies the level of integrin $\alpha_v\beta_3$ expression in man. *Clin. Cancer Res.* **2006**, *12* (13), 3942–9.

(5) Haubner, R.; Weber, W. A.; Beer, A. J.; Vabuliene, E.; Reim, D.; Sarbia, M.; Becker, K. F.; Goebel, M.; Hein, R.; Wester, H. J.; Kessler, H.; Schwaiger, M. Noninvasive visualization of the activated $\alpha_v\beta_3$ integrin in cancer patients by positron emission tomography and [^{18}F]Galacto-RGD. *PLoS Med.* **2005**, *2* (3), e70.

(6) Kenny, L. M.; Coombes, R. C.; Oulie, I.; Contractor, K. B.; Miller, M.; Spinks, T. J.; McParland, B.; Cohen, P. S.; Hui, A. M.; Palmieri, C.; Osman, S.; Glaser, M.; Turton, D.; Al-Nahhas, A.; Aboagye, E. O. Phase I trial of the positron-emitting Arg-Gly-Asp (RGD) peptide radioligand ^{18}F-AH111585 in breast cancer patients. *J. Nucl. Med.* **2008**, *49* (6), 879–86.

(7) Janssen, M. L.; Oyen, W. J.; Dijkgraaf, I.; Massuger, L. F.; Frielink, C.; Edwards, D. S.; Rajopadhye, M.; Boonstra, H.; Corstens, F. H.; Boerman, O. C. Tumor targeting with radiolabeled alpha(v)beta(3) integrin binding peptides in a nude mouse model. *Cancer Res.* **2002**, *62* (21), 6146–51.

(8) Yoshimoto, M.; Ogawa, K.; Washiyama, K.; Shikano, N.; Mori, H.; Amano, R.; Kawai, K. alpha(v)beta(3) Integrin-targeting radionuclide therapy and imaging with monomeric RGD peptide. *Int. J. Cancer* **2008**, *123* (3), 709–15.

(9) Haubner, R.; Decristoforo, C. Radiolabelled RGD peptides and peptidomimetics for tumour targeting. *Front. Biosci.* **2009**, *14*, 872–86.

(10) Liu, S. Radiolabeled cyclic RGD peptides as integrin alpha-(v)beta(3)-targeted radiotracers: maximizing binding affinity via bivalency. *Bioconjugate Chem.* **2009**, *20* (12), 2199–213.

(11) Wu, Y.; Zhang, X.; Xiong, Z.; Cheng, Z.; Fisher, D. R.; Liu, S.; Gambhir, S. S.; Chen, X. microPET imaging of glioma integrin {alpha}v{beta}3 expression using ^{64}Cu-labeled tetrameric RGD peptide. *J. Nucl. Med.* **2005**, *46* (10), 1707–18.

(12) Liu, Z.; Liu, S.; Wang, F.; Liu, S.; Chen, X. Noninvasive imaging of tumor integrin expression using ^{18}F-labeled RGD dimer peptide with PEG_4 linkers. *Eur. J. Nucl. Med. Mol. Imaging* **2009**, *36* (8), 1296–307.

(13) Shi, J.; Wang, L.; Kim, Y. S.; Zhai, S.; Liu, Z.; Chen, X.; Liu, S. Improving tumor uptake and excretion kinetics of ^{99m}Tc-labeled cyclic arginine-glycine-aspartic (RGD) dimers with triglycine linkers. *J. Med. Chem.* **2008**, *51* (24), 7980–90.

(14) Shi, J.; Kim, Y. S.; Zhai, S.; Liu, Z.; Chen, X.; Liu, S. Improving tumor uptake and pharmacokinetics of ^{64}Cu-labeled cyclic RGD peptide

dimers with Gly_3 and PEG_4 linkers. *Bioconjugate Chem.* **2009**, *20* (4), 750–9.

(15) Wang, L.; Shi, J.; Kim, Y. S.; Zhai, S.; Jia, B.; Zhao, H.; Liu, Z.; Wang, F.; Chen, X.; Liu, S. Improving tumor-targeting capability and pharmacokinetics of ^{99m}Tc-labeled cyclic RGD dimers with PEG_4 linkers. *Mol. Pharmaceutics* **2009**, *6* (1), 231–45.

(16) Liu, Z.; Liu, S.; Niu, G.; Wang, F.; Liu, S.; Chen, X. Optical imaging of integrin $\alpha_v\beta_3$ expression with near-infrared fluorescent RGD dimer with tetra(ethylene glycol) linkers. *Mol. Imaging* **2010**, *9* (1), 21–9.

(17) Liu, S. Radiolabeled cyclic RGD peptides as integrin $\alpha_v\beta_3$-targeted radiotracers: maximizing binding affinity via bivalency. *Bioconjugate Chem.* **2009**, *20* (12), 2199–213.

(18) Liu, Z.; Li, Z. B.; Cao, Q.; Liu, S.; Wang, F.; Chen, X. Small-animal PET of tumors with ^{64}Cu-labeled RGD-bombesin heterodimer. *J. Nucl. Med.* **2009**, *50* (7), 1168–77.

(19) Li, Z. B.; Cai, W.; Cao, Q.; Chen, K.; Wu, Z.; He, L.; Chen, X. 64)Cu-labeled tetrameric and octameric RGD peptides for small-animal PET of tumor alpha(v)beta(3) integrin expression. *J. Nucl. Med.* **2007**, *48* (7), 1162–71.

(20) Shi, J.; Kim, Y. S.; Chakraborty, S.; Zhou, Y.; Wang, F.; Liu, S. Impact of bifunctional chelators on biological properties of 111In-labeled cyclic peptide RGD dimers. *Amino Acids* **2010**Epub ahead of print.

(21) Chakraborty, S.; Shi, J.; Kim, Y. S.; Zhou, Y.; Jia, B.; Wang, F.; Liu, S. Evaluation of 111In-labeled cyclic RGD peptides: tetrameric not tetravalent. *Bioconjugate Chem.* **2010**, *21* (5), 969–78.

(22) Janssen, M.; Oyen, W. J.; Massuger, L. F.; Frielink, C.; Dijkgraaf, I.; Edwards, D. S.; Radjopadhye, M.; Corstens, F. H.; Boerman, O. C. Comparison of a monomeric and dimeric radiolabeled RGD-peptide for tumor targeting. *Cancer Biother. Radiopharm.* **2002**, *17* (6), 641–6.

(23) Dijkgraaf, I.; Kruijtzer, J. A.; Liu, S.; Soede, A. C.; Oyen, W. J.; Corstens, F. H.; Liskamp, R. M.; Boerman, O. C. Improved targeting of the alpha(v)beta (3) integrin by multimerisation of RGD peptides. *Eur. J. Nucl. Med. Mol. Imaging* **2007**, *34* (2), 267–73.

(24) Wu, Y.; Zhang, X.; Xiong, Z.; Cheng, Z.; Fisher, D. R.; Liu, S.; Gambhir, S. S.; Chen, X. microPET imaging of glioma integrin {alpha}v{beta}3 expression using (64)Cu-labeled tetrameric RGD peptide. *J. Nucl. Med.* **2005**, *46* (10), 1707–18.

(25) Liu, Z.; Jia, B.; Shi, J.; Jin, X.; Zhao, H.; Li, F.; Liu, S.; Wang, F. Tumor Uptake of the RGD Dimeric Probe ^{99m}Tc-G_3-$2P_4$-RGD2 is Correlated with Integrin $\alpha_v\beta_3$ Expressed on both Tumor Cells and Neovasculature. *Bioconjugate Chem.* **2010**, *21*, 548–55.

(26) Liu, Z.; Jia, B.; Zhao, H.; Chen, X.; Wang, F. Specific targeting of human integrin $\alpha_v\beta_3$ with ^{111}In-labeled Abegrin^{TM} in nude mouse models. *Mol. Imaging Biol.* **2011**, *13* (1), 112–20.